EXAMINATION OF NANO-C60 AGGREGATES THROUGH DIALYSIS MEMBRANES AS SURROGATES FOR CELL MEMBRANE DIFFUSION

By

KELLY LOOKABILL STUMP

**A thesis submitted in partial fulfillment of
the requirements for the degree of**

Master of Science in Environmental Science

**WASHINGTON STATE UNIVERSITY
School of Earth and Environmental Sciences**

DECEMBER 2009

To the Faculty of Washington State University:

The members of the Committee appointed to examine the thesis of KELLY LOOKABILL STUMP find it satisfactory and recommend that it be accepted.

_____

Allan S. Felsot, Ph.D., Chair

_____

A. Scott Lea, Ph.D.

_____

Chongmin Wang, Ph.D.

ACKNOWLEDGMENT

This thesis would not have been possible without the support of my committee, Dr. Allan Felsot, Dr. A. Scott Lea and Dr. Chongmin Wang. Without their willingness to schedule time to instruct me on how to be a better scientist I wouldn't have been able to acquire this degree. I would also like to thank the User program and the Environmental Molecular Sciences Laboratory at the Pacific Northwest National Laboratory for allowing the use of the instruments and the time to use them. To Battelle, my employer, for the financial support and the time flexibility needed to acquire this degree. And to my family for always supporting any new endeavor I choose to pursue.

EXAMINATION OF NANO-C60 AGGREGATES THROUGH DIALYSIS MEMBRANES AS SURROGATES FOR CELL MEMBRANE DIFFUSION

Abstract

by Kelly Lookabill Stump
Washington State University
December 2009

Chair: Allan S. Felsot

Nanoparticles in the environment are naturally ubiquitous but the increased introduction of nanoscale materials may have unintended ecotoxicological effects. One nanoparticle produced in large quantities is buckminsterfullerene or C60. Studies confirmed the formation of C60 aggregates (nano-C60) as C60 come into contact with water. Suspensions of nano-C60 may also have ecotoxicological properties. Studies have shown that C60 and nano-C60 cause cellular membrane stress, lipid peroxidation of the phospholipid bilayer, and readily move into the cell. Conversely, another study showed that C60's do not penetrate into the lipid bilayer because they adsorb to the hydrophilic functional groups.

Whether nano-C60 has potential for toxicological effects depends on whether nano-C60 can diffuse through membranes. Because of the conflicting observations of nano-C60 interactions with a phospholipid bilayer, this study proposed using dialysis membranes as surrogates for cellular membranes. Use of dialysis membranes reduces the question

of cellular toxicity interaction to one aspect of toxicological properties, what size nanoparticles can diffuse through pores in cells.

A bulk suspension of nano-C60 was produced and dialysis cells of variable pore size were used to determine if nano-C60 was diffusing into the interior water. UV/Visible spectrophotometry, atomic force microscopy, and transmission electron microscopy techniques examined the aggregate formation in the bulk solution and within the dialysis membranes. Particle sizes tended to increase in direct proportion to dialysis membrane pore size. The particles were larger than expected based on pore size, but C60 aggregation may have continued inside the cells. Some AFM images unexpectedly contained lines swirled around the particles recovered from dialysis cells but not surrounding particles in the bulk suspension. TEM images did not show any line formation but the TEM does not have the resolution of the AFM due to the grid it is prepared upon.

The experiment showed the smallest dialysis pores effectively reduced diffusion of nano-C60. This observation suggests that environmental exposures to nano-C60 won't necessarily lead to bioavailability because plasma membrane pore diameters are likely smaller than the dialysis pores that effectively excluded buckyball diffusion. But if increased pore size is occurring due to cellular rupture, diffusion rate would then become important.

TABLE OF CONTENTS

LIST OF TABLES

List of Figures

Dedication

To my husband, Brent, for always listening to all my ideas and ramblings. I have loved our last 20 years together and look forward to the next 20 years together.

Introduction

Natural and man-made, nanoparticles are ubiquitous in the environment. Colloids, such as clays and minerals, have been studied in soils and waters while sea salt, wildfire smoke and diesel particulates have been studied in the air. Surface chemists have long studied the nanostructure of shells and material surfaces. But the ability to manipulate, and therefore mass produce, nanomaterials has recently greatly increased and so has the quantities introduced into the environment. The increased introduction of large quantities of nanoparticles into the environment may have unintended effects and their environmental chemistry and ecotoxicological properties need to be studied in greater depth.

To determine the toxicological properties of nanomaterials, several aspects of the nanoparticle must be taken into consideration. Studies on the cellular toxicity of carbon based nanomaterials have shown that form, size, aspect ratio, and surface charge all influence toxicity (Magrez et al., 2006).

One such nanoparticle that has been studied for decades and that is currently being produced in large quantities is buckminsterfullerene, commonly known as C60. This carbon allotrope differs from other carbon allotropes, such as graphite, diamonds, and amorphous carbon because it is a finite structure. C60 consists of sixty carbon atoms bonded together to form a hollow sphere approximately 1 nanometer in size (Kroto, et al., 1985).

Studies have confirmed the natural formation of C60 aggregates, nano-C60, as C60 comes into contact with water (Fortner et al., 2005). The nano-C60 forms both crystalline and amorphous colloidal structures in water. Oberdorster indicates in 2006 that nano-C60's can be taken up by organisms from water; suggesting diffusion across membranes is a reasonable route for bioavailability.

This study measured the diffusion of nano-C60 aggregates through dialysis cells used as surrogates for cell membranes consisting of different pore sizes. The hypothesis is that diffusion potential of nanoparticle aggregates across membranes is related to dialysis cell pore size. This hypothesis would predict that exposing the nano-C60 aggregates to increasingly smaller dialysis cell pore sizes will filter the nanoparticles from entering the cell. This will help determine one aspect of toxicological properties, what size nanoparticles and its aggregates can pass through pores in cells.

BACKGROUND AND LITERATURE REVIEW

In 1985, the C60 structure was deduced (Kroto, et al., 1985). The mass production of C60 began in 1991 and in 1996 the Nobel Prize was presented to Smalley, Kroto and Curl for the discovery of the first structure in the fullerene family (Nobelprize.org, 1996). Analytical chemists and theoreticians have since determined the chemistry of the C60 nanoparticle and have used this knowledge to help predict C60 interactions.

Structure and Chemistry

C60 is a modified icosahedron. An icosahedron is a regular polyhedron having 20 identical equilateral triangular faces with 12 identical vertices (Figure 1a). C60 is a truncated icosahedron with a pentagon replacing each of the 12 identical vertices in the icosahedron. The truncation creates 12 new pentagon faces and turns the original 20 triangular faces into 20 regular hexagons with edge lengths one third of the original edge (Kroto, et. al, 1991). This creates a structure with 60 vertices (Figure 1b). Each vertice represents a carbon atom in the C60 structure.

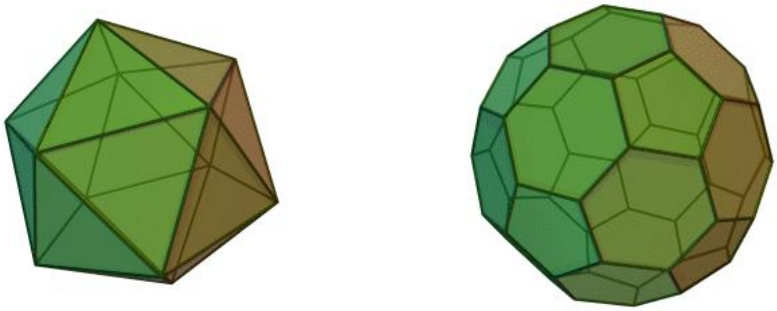

Figure 1. Structure of polyhedrons. Figure 1a: Structure of a regular icosahedron; Figure 1b: Structure of the truncated icosahedron

URL: http://en.wikipedia.org/wiki/Icosahedron

http://en.wikipedia.org/wiki/Truncated_icosahedron

C60 therefore has twelve pentagons and twenty hexagons in a stable caged shape. Twelve pentagons are required for closure of the sphere and C60 is the first stable fullerene because it is the smallest possible number of carbons to obey this rule and thus not allow any of the pentagons to come into contact with one another. This

structural arrangement is called the isolated pentagon rule (IPR) which holds that all naturally occurring fullerenes have isolated pentagons (Kroto, et. al, 1991).

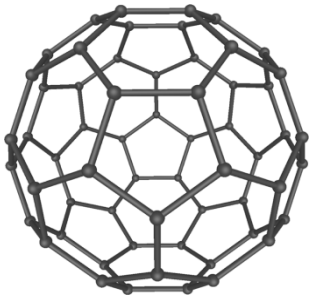

Figure 2: C60 Buckyball structure URL: http://en.wikipedia.org/wiki/File:C60a.png

There are two types of bonds in the fullerene structure. The pentagons form single bonds and the hexagons form double bonds. The electrons of the C60 molecule therefore form a conjugated system with delocalized pi double bond systems over the hexagons. This double bond structure lowers the required energy needed to form a bent cage structure. Although the C60 structure is relatively stable and inert, the entire structure does not exhibit 'superaromaticity' because the electrons do not delocalize over the pentagon carbons (Kroto, et. al, 1991).

Because of the spherical shape of buckyballs the carbon atoms are forced into a trigonal planar structure rather than the less strained tetrahedral shape. The sp^2-hybridized, or trigonal planar, carbons atoms are bent to form the sphere-like structure and therefore show slight angle strain. The electrophilic addition at the 6,6-double bonds reduces angle strain by changing the trigonal planar carbons back into sp^3-hybridized, or tetrahedral, atoms. As a result, C60 can be considered slightly electrophilic (Locke. 1996). The conjugated carbon atoms of the hexagons respond to

deviation from planarity by orbital rehybridization with a gain in p-character. The pi lobes extend further outside the surface than they do into the interior of the sphere and this causes the sphere to be electronegative (Locke. 1996).

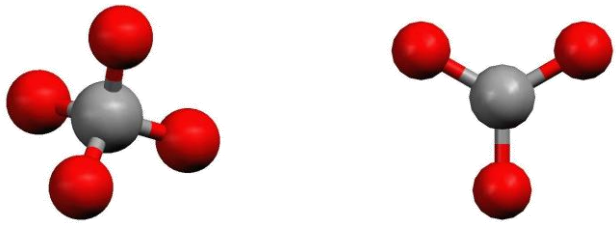

Figure 3: Tetrahedral and trigonal planar structures observed in fullerenes

URL: http://chemlab.truman.edu/CHEM121Labs/MolecularModeling1.htm

When originally studied, C60 nanoparticles unexpectedly formed organic aggregates in an aqueous media. Later studies showed the higher surface energy and electrophilic properties of C60 nanoparticles cause strong interactions with each other to form colloidal aggregates (Andrevsky et al., 1999). Essentially, the organic structure of the formed nano-C60 aggregates contains a negative surface charge and behaves as a stable nanoparticle suspension or colloid (Alargova et. al., 2001).

The isoelectric point (pI), the pH at which a surface carries no net electrical charge, of aqueous colloidal suspensions of stable fullerene aggregates was <1.0 (Bouchard, D; et. al., 2009). The pI value affects the solubility of a molecule at a given pH. The pH of the suspensions generated was 3.75, which are conceivably found in nature, and formed the most colloids and crystalline structures possible.

Ecotoxicology

Based on the previously determined chemistry of the C60 structure, it would be presumed that a partial negative charge on a structure would not allow direct diffusion across a phospholipid bilayer. But subsequent studies have shaped various opinions about the effect that C60 and its colloidal aggregates, nano-C60, have on cellular structure. Early studies by Hungerbuhler et al. (1993) showed that the incorporation of a singular C60 into an artificial lipid membrane could allow for electron transport across the lipid bilayer. Kamat et al. (2000) showed that a reactive oxygen species was formed at the cellular membrane and caused fullerene induced oxidative damage. Sayes et al. (2004) showed that water-soluble C60 aggregates (nano-C60) also caused lipid peroxidation and membrane damage in human cells.

Studies confirmed the natural formation of C60 aggregates as singular C60 comes into contact with water in the environment (Fortner et al., 2005). For the first time, microbial response following exposure to C60 aggregates was observed. Others have noted potential ecotoxicological concerns based on toxicological studies with aquatic organisms (Oberdorster et al., 2005).

Aggregation rate, structure and morphology of nano-C60 were determined to help assess ecological risk associated with aqueous exposure (Fortner et. al, 2005). Although C60 is initially insoluble in water, it can be suspended through a couple of different methods and the formation of nano-C60 aggregates is affected by solution chemistry. In particular, a slow rate of water addition and a low pH of the suspension

cause the highest rate of aggregation and also affect the size and shape of the aggregates during formation. Nano-C60 aggregates vary in size from 10 nm to 300 nm in diameter and form multiple shapes (Fortner et al., 2005).

Further studies show that C60 and its aggregates cause cellular membrane stress and disruptive effects in microbial structural integrity (Tang et al., 2007). Cell membrane damage was shown to occur by lipid peroxidation of the phospholipid bilayer (Sayes et al., 2005). Evidence for C60 and nano-C60 production of oxygen radicals resulting in lipid peroxidation and thus allowing access into the cell was shown by Dhawan in 2006. This access increases the bioavalibility of the C60 and nano-C60 possibly allowing for genotoxicity and cytoplasmic membrane damage by the solubilized fullerenes (Dhawan et al., 2006). Modelling has shown that C60 readily jump into the membrane and could cross a lipid bilayer (Qiao et al., 2007). Conversely, another study showed that nano-C60 could not penetrate into the hydrocarbon tails of a supported bilayer because they absorb to the hydrophilic functional groups (Spurlin et al., 2007).

The production of C60 and its introduction into the environment causes possible routes of exposure through both dermal and oral routes. The bioavailability of the nano-C60 then becomes a concern because of the possible interactions with cellular membranes. Because of the conflicting observations of nano-C60 interactions with a phospholipid bilayer this study was designed to examine nano-C60 diffusion through dialysis cells as surrogates for cell membranes. Use of dialysis membranes can eliminate the question of toxic interactions with cells and focus on one aspect of toxicological properties, what

size nanoparticles and its aggregates can diffuse through pores in cells. Once it is understood what pore size allows diffusion across the cellular membrane, further studies would then incorporate the peroxidation of the membrane to cause potentially increased pore size.

Route of Exposure

Dialysis cell pore sizes were chosen to represent a range of pore sizes that would occur in cell membranes. Aquaporins, the route that cells selectively allow water to the interior and exclude ions, are typically <1 nm diameter (Nobelprize.org , 2003) and singular fullerenes are about 1 nm in diameter. The smallest dialysis pore used was therefore ~1 nm. Aquaporins could conceivably be a route of exposure for the fullerenes into the cells.

As noted in other studies, conditions of stress can cause membrane pore size to rapidly increase. For example conditions of lipid peroxidation (Dhawan, 2006) or the presence of bacterial toxins (Clinkenbeard et al. 1989) could cause significant membrane pore size changes. The largest dialysis pore size was ~100 nm to account for the possibility that cell membranes under stress may allow diffusion of the nano-C60 aggregates. The 100 nm size was also chosen because the aggregate material is no longer considered nanoscale material above 100 nm as it begins to lose the novel properties it had at the nanoscale level. Therefore, small and large pore sizes were used to examine the method of entry for nano-C60 into the cells.

RESEARCH DESIGN AND METHODOLOGY

The design of this experiment was to study one aspect of the nano-C60 suspension, the diffusion of particulates through cellular membranes. The movement of colloids across membranes can be passive, occurring without the input of cellular energy, or active, requiring the cell to expend energy for transport. Because specialized transmembrane proteins have evolved for active transport processes, any incorporation of xenobiotic contaminants are most likely to occur through diffusion. Contaminants therefore either passively diffuse across lipid bilayers or move through transmembrane pores.

Based on simulation studies (Qiao et al. 2007), pristine C60 has the potential to “jump” into the lipid bilayer, while the larger aggregates would be repelled. However, once in the bilayer, C60 may not diffuse out again but the formation of micropores could facilitate further transport (Qiao et al. 2007). But if the chemistry of the C60 nanoparticle accounts for the peroxidation effects that potentially causes ruptures in the membrane, then the filtering capacity of the cell pores in membranes is an important aspect to study to understand bioavailability of nano-C60 particulates.

Setting up dialysis cells as surrogates for cell membrane allowed diffusion through pores to be the only process for entering the cell. Different size pore membranes were then used to determine when the aggregates would filter through the cellular membrane.

Experiment Objectives

This experiment examined the movement of C60 and the aggregates, nano-C60, formed under ambient conditions of the laboratory through dialysis cells that served as surrogates for cell membrane diffusion. The objective of using dialysis membranes was to determine how effectively pore size would influence transmembrane movement and thus predict how permeable cells might be to different nano-C60 aggregate sizes. The composition of the bulk suspension surrounding the membranes was based on a previously published study showing prolific nano-C60 aggregate formation at a pH of 3.75 and suspension mixing rate of 300 rpm (Fortner, et. al, 2005).

Experimental Setup

The experiment was set up using the dialysis pore size as the independent variable, the filtration of the formed nanoparticles as the dependent variable and the pH and the mixing rate as the controlled variables.

Methods and Materials

Dialysis membranes filled with deionized were used to study the diffusion potential of buckyball aggregates in an aqueous suspension. Dialysis membranes were placed in a suspension of buckyball aggregates and after twenty days, the water inside the dialysis cell was analyzed by UV/Vis to determine the concentration of nano-C60. Particle sizing and visualization were then performed by atomic force microscopy (AFM) and transmission electron microscopy (TEM). Particle size analysis was used to determine if nano-C60 concentration varied among dialysis membranes of differing pore sizes.

Preparation of C60 in Water:

Approximately 200 mg of C60 (99.5% pure) purchased from SES Research (SES Research, 2009) was added to 1L of HPLC grade water acidified to a pH of 3.75 with hydrochloric acid. The water/fullerenes were stirred using a bench-top magnetic stirrer at 300 rpm for 30 days under constant tungsten light. At the end of the 30 days, the larger aggregates of un-dispersed fullerenes were removed by centrifugation at 5000 x g for 20 minutes each time. After each spin, the supernatant was decanted and then subjected to centrifugation and decanting for a total of three cycles. The supernatant after the final centrifugation yielded a clear liquid indicating removal of undispersed fullerene clumps.

Preparation of Dialysis cells in Water:

After the aggregate suspension had been mixed, dialysis cell sample preparation was accomplished by utilizing stand-alone dialysis cells of various pore sizes filled with deionized water (Spectrum Laboratories, Rancho Dominguez, Ca.). The dialysis membrane pore sizes were 0.5 kDalton (kD) or ~ 1 nanometer (nm), 3.5-5 kD (~7 to 10 nm), 20 kD (~40 nm), and 50 kD (~100 nm). The water-filled cells were placed in C60 buckyball aggregate suspension contained in a large 1-L beaker that was placed on a magnetic stir bar mixer operated at a rate of ~ 300 rpm. A blank bulk solution with dialysis membrane cells was similarly prepared using DI water acidified with hydrochloric acid to a pH of 3.75 in a 1-L beaker. Dialysis cells of all pore sizes were

placed together in the same bulk suspension to ensure that all were exposed to the same nano-C60 aggregate concentrations.

The dialysis cells stirred in the bulk suspension for 4 weeks. The cells were then removed and the internal water pipetted into sample containers. The containers were then packaged for transport and analysis at the Environmental Molecular Sciences Laboratory (EMSL), Richland, Washington.

Analytical Techniques

To visualize nanoparticulates several analytical techniques were utilized to understand the interactions of the nano-C60 from different views. UV/Visible photometry (UV/Vis) was used to determine an estimated concentration of the nano-C60 in suspension and if the aggregates had breached the cellular membranes. Atomic Force Microscopy (AFM) was used to produce three-dimensional images. Size, shape, and particle count can be conducted on selected by the operator as areas of interest. Transmission Electron Microscopy (TEM) was used to produce a diffraction pattern of singular clusters of nanoC60 aggregates. The diffraction pattern is used to form a clear image of the sample. The diffraction pattern can also be used to distinguish between crystalline and amorphous samples.

UV/Visible Spectrophotometry (UV/VIS)

To determine if the C60 were forming colloids, the suspension was measured by UV/Vis after it was oxidized by the addition of a 2:1 ratio of bleach. Bleach at a concentration of

50 mg/L was added to the nano-C60 sample, (1 ml of nano-C60 suspension and 2 ml of Clorox brand unscented bleach). The sample was then vortexed vigorously once a minute for 20 seconds for 10 minutes. To extract the oxidized nano-C60, 1 ml of toluene was added. The aqueous organic suspension was then vortexed vigorously once a minute for 20 seconds for 15 minutes. The top 1 ml of toluene was pipetted and centrifuged at 14,000 x g for 5 minutes. The absorbance of the supernatant was read at 336 nm in quartz cuvettes (Nanotox.info, 2008).

Concentration of the nano-C60 samples was determined from a calibration curve from UV/VIS analysis. Standards were produced by dissolving 25 mg of C60 (99.5% pure) purchased from SES Research in toluene. A regression curve was generated from the standards absorbance unit readings, see Figure 4. The known concentrations were then used to determine a concentration of the unknown samples and blanks.

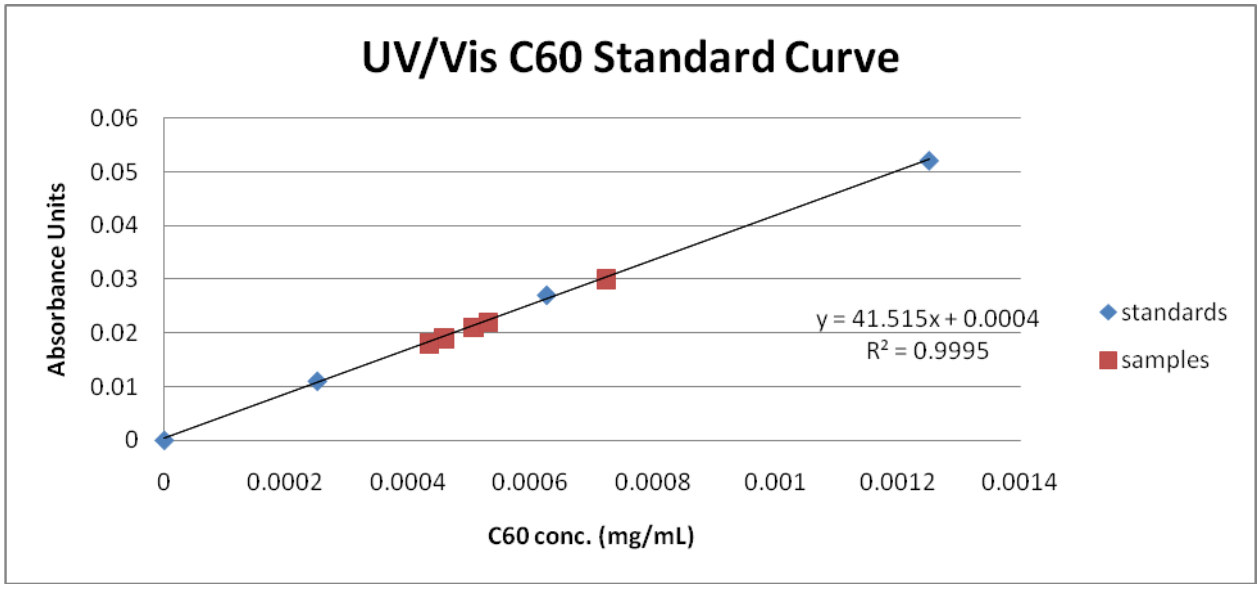

Figure 4: Calibration curve for incremental concentrations of C60.

The regression equation was used to calculate the concentrations of unknown samples.

Atomic Force Microscopy

Atomic force microscopy (AFM) is a technique used for imaging. A cantilever with a sharp probe is used to scan the sample surface. A laser beam is situated on top of the cantilever and the forces between the sample and the tip cause the cantilever to be deflected. The deflection is measured by a photodiode to determine movement and image the geometry of the structures. This produces a three-dimensional image of the surface. Advantages are three dimensional (length, width, and height) measurements, good resolution at ambient environmental conditions and little sample preparation. Disadvantages include long scan time, sample interference, and tip resolution issues. Tip resolution issues with a misshapen tip can create possible artifacts and increase observed sample dimensions (Nanosciences Instruments, 2008).

A circular piece of mica was punched out for use as a substrate to support the sample and the mica was sliced in half to obtain a clean and smooth edge. The sample was then inverted for ten seconds to disperse the buckyballs. One drop of sample suspension was then placed on the mica and dried for 12 hours.

Transmission Electron Microscopy

Transmission electron microscopy is a technique used for imaging where a beam of electrons is focused and transmitted through a sample and a diffraction pattern is magnified and captured. The diffraction pattern is then used to form an image of the sample. Advantages are clear images with good resolution and sharp contrast, easy to

scan then focus on clusters, and ability to differentiate between crystalline and amorphous structures. Disadvantages include the sample preparation to ensure a sample thin enough for transmission and it is a two dimensional analysis (Nobelprize.org, 2009).

The sample was inverted for ten seconds to disperse the buckyballs. One drop of sample suspension was placed on a titanium metal grid and dried for 2 minutes.

Microscopy of Bulk and Dialysis Cell Suspensions

The following pages are images of the samples produced by AFM and TEM analysis. The TEM images provide information about shape and size of the aggregate formed in the dialysis cells. The TEM diffraction patterns indicate whether the particle was amorphous or crystalline. A particle analysis of the AFM images was performed by the AFM Nanoscope software provided with the instrument. This supplied information about the particle number count and particle size. Two particle analyses were performed, the first with a threshold height (particle height cut off) of 1 nm and the second with a threshold height of 2 nm. The use of the two threshold heights was to compare results from the cutoff point of one C60 buckyball, approximately 1 nm in height, and nano-C60 aggregates which would be 2 nm in height or higher.

Results

UV/Vis spectrophotometry was used to confirm the presence of C60 in the samples. A DI blank and blank composed of bleach water were tested and an absorbance reading higher than the toluene blank was noted. The suspensions collected from inside the dialysis membranes were analyzed, and with the exception of the suspension from the 20 kD membrane, all had slightly higher absorbance readings than the readings in the bleach blank. This indicated diffusion into the dialysis membranes. The original C60 bulk suspension, taken before the dialysis cells were added and preserved in the refrigerator, was about the same concentration as the suspensions taken from inside the dialysis cells and slightly higher than the blanks. The C60 aggregate bulk suspension taken after spinning with the dialysis cells was noticeably higher then C60 aggregate bulk suspension preserved in the refrigerator (Table 1). This observation suggests that the suspension in the beaker continued to form aggregates while spinning with the dialysis cells.

Table 1: Calculated concentrations of nano-C60 samples taken from bulk suspension and inside of dialysis cells.

Sample	**UV/Vis Absorbance Units**	**mg/mL** [1/]
DI blank	0.018	0.000434
Bleach blank	0.018	0.000434
C60 original aggregate suspension	0.021	0.000506
C60 aggregate suspension after spinning	0.030	0.000723
Suspension inside 0.5 kD	0.021	0.000506
Suspension inside 5 kD	0.019	0.000458
Suspension inside 20 kD =	0.018	0.000434
Suspension inside 50 kD =	0.022	0.000530

[1/] Calculations were based on the calibration curve equation, y = 41.51x, determined from regression analysis (Figure 1).

Replicate analyses were then performed by AFM and TEM for each dialysis cell samples along with the blank and bulk aggregate samples.

Visual Inspection

From the initial visual inspection of the images, it is noticed that the 0.5 kD dialysis cell sample contains what appears to be false images most probably caused by tip resolution issues (Figure 5). A misshapened or dull tip can cause streaky images when encountering small particles and thin lines will be analyzed as particles. The thin lines then disproportionately change the particles analysis grain size and the results would therefore be skewed. The 0.5 kD sample was the first sample analyzed and it was not noticed that this was an issue. The sample tips are routinely changed and only upon inspection did the results look skewed.

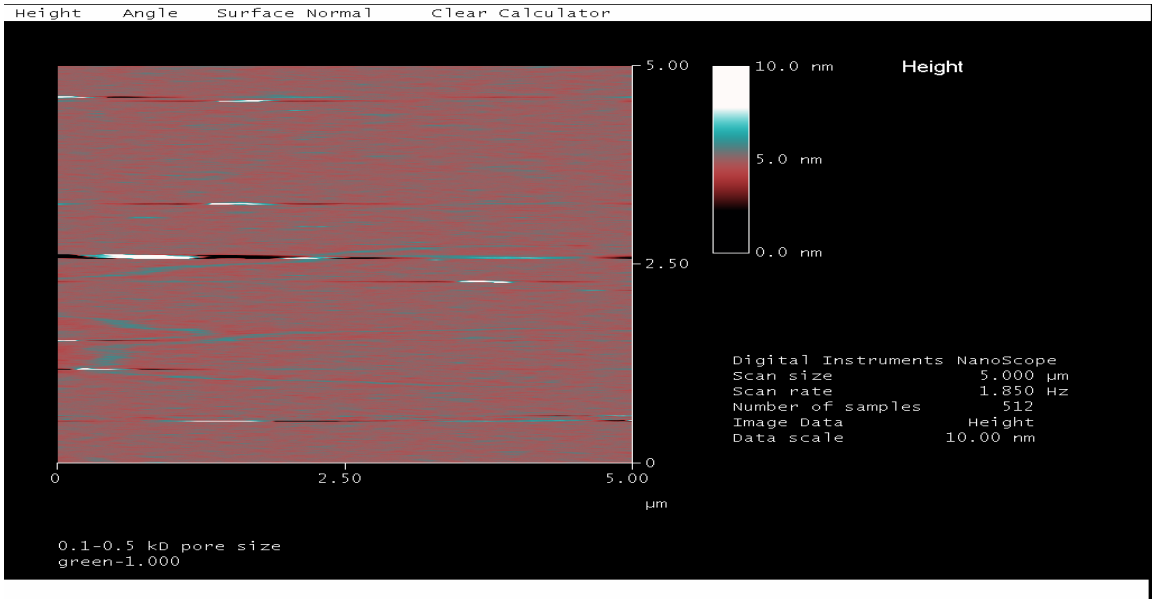

Figure 5: Image from atomic force microscopy (AFM) analysis of a sample from a 0.5 kD dialysis cell. The image shows clear streaking across the field of view. Perspective looks down from the top of particles 10 nm height.

The observation of streaking confounds interpretation of the results; therefore, the 0.5 kD sample are therefore not considered in the comparisons. The TEM images do show amorphous and crystalline structures that have formed, but they were not found during the AFM scan. It is easier to find images with a TEM, but particle analysis cannot be performed. The difference in observations of particles between the TEM and AFM images suggested that buckyballs diffused into the dialysis cells but were not widely dispersed (Figure 6).

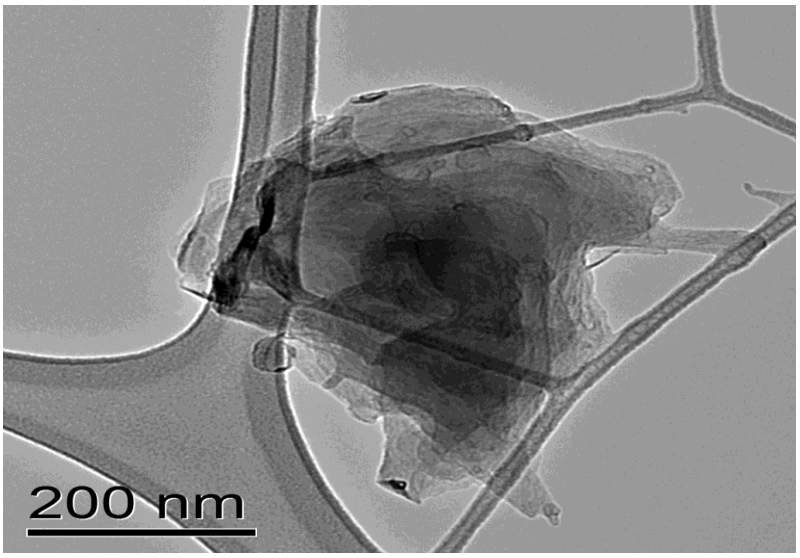

Figure 6: Transmission electron micrograph (TEM) of a nano-C60 aggregate extracted from a sample of the 0.5 kD dialysis cell.

The visual inspection revealed unusual formations in the AFM images. The formation of swirling lines is seen in the 5 kD dialysis sample cell images that are not seen in the blank or in the bulk samples (Figure 7-9).

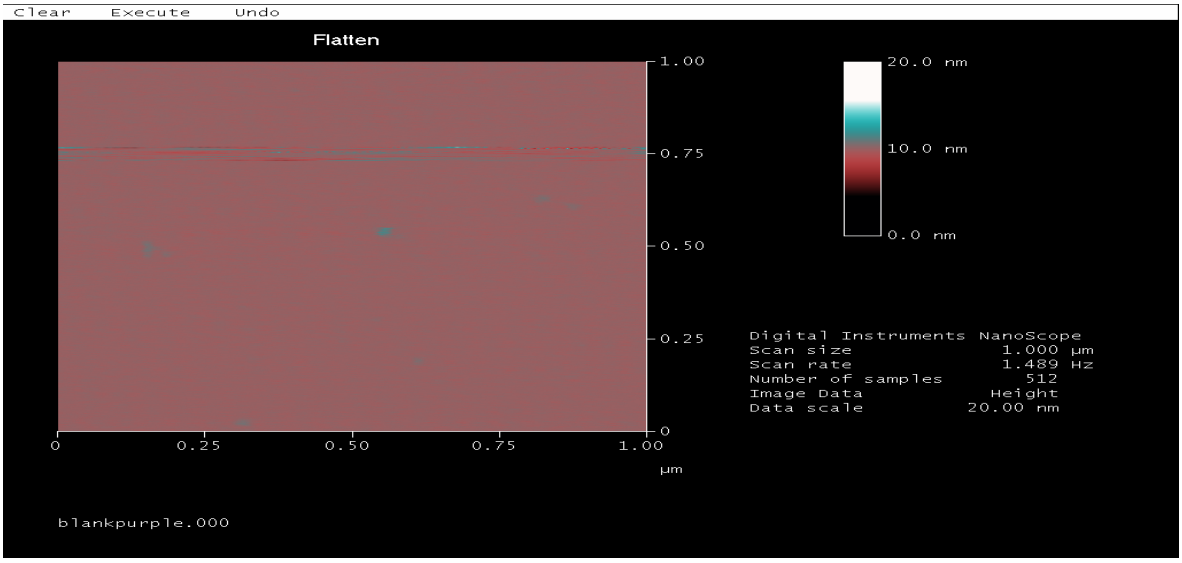

Figure 7. Image from atomic force microscopy (AFM) analysis of a blank sample from a 50 kD dialysis cell. Perspective looks down from the top of particles 20 nm height.

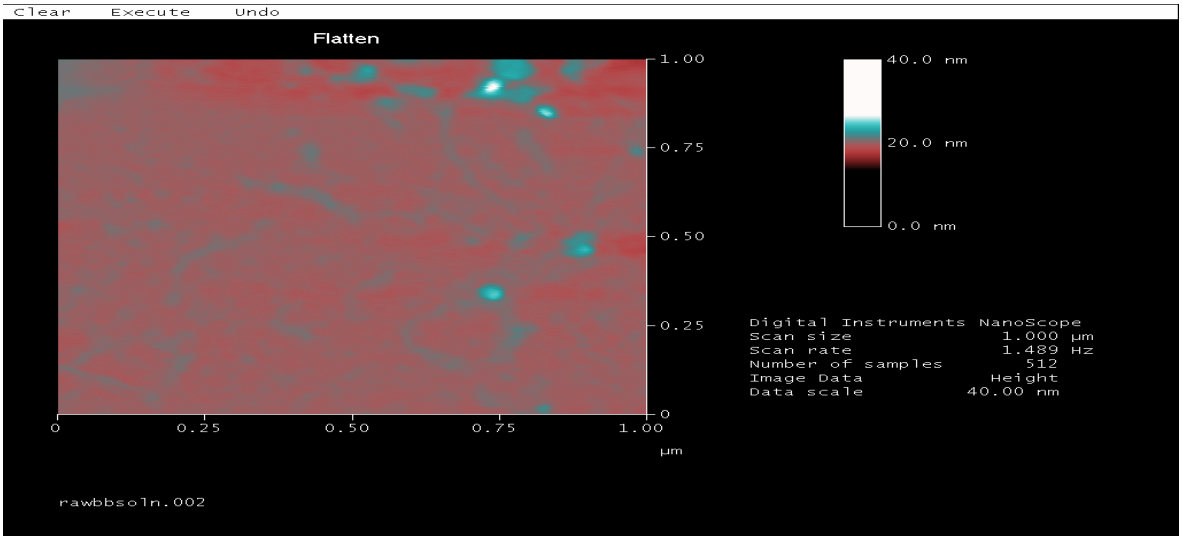

Figure 8. Image from atomic force microscopy (AFM) analysis of a bulk suspension sample. Perspective looks down from the top of particles 40 nm height.

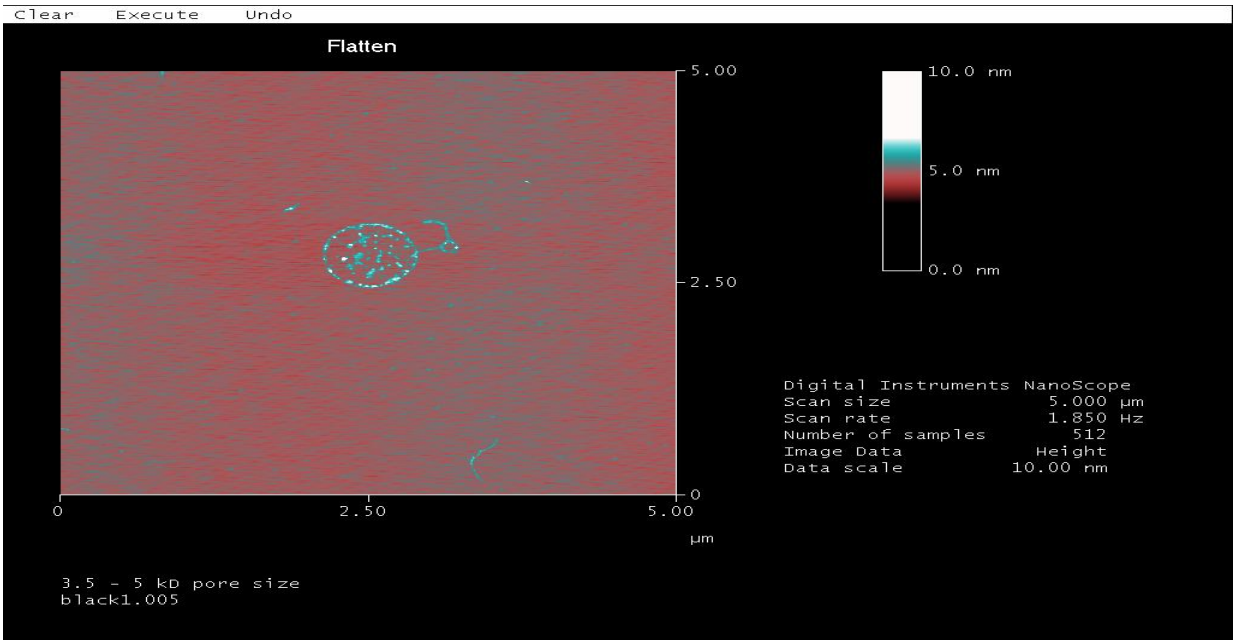

Figure 9. Image from atomic force microscopy (AFM) analysis of a sample from a 5 kD dialysis cell. Perspective looks down from the top of particles 10 nm height.

In the 20 kD and the 50 kD dialysis cell images the swirling lines extend from the larger particles in the sample suspension (Figures 10 - 11). This has not been seen before in particle analysis literature and was unique to the dialysis cell samples.

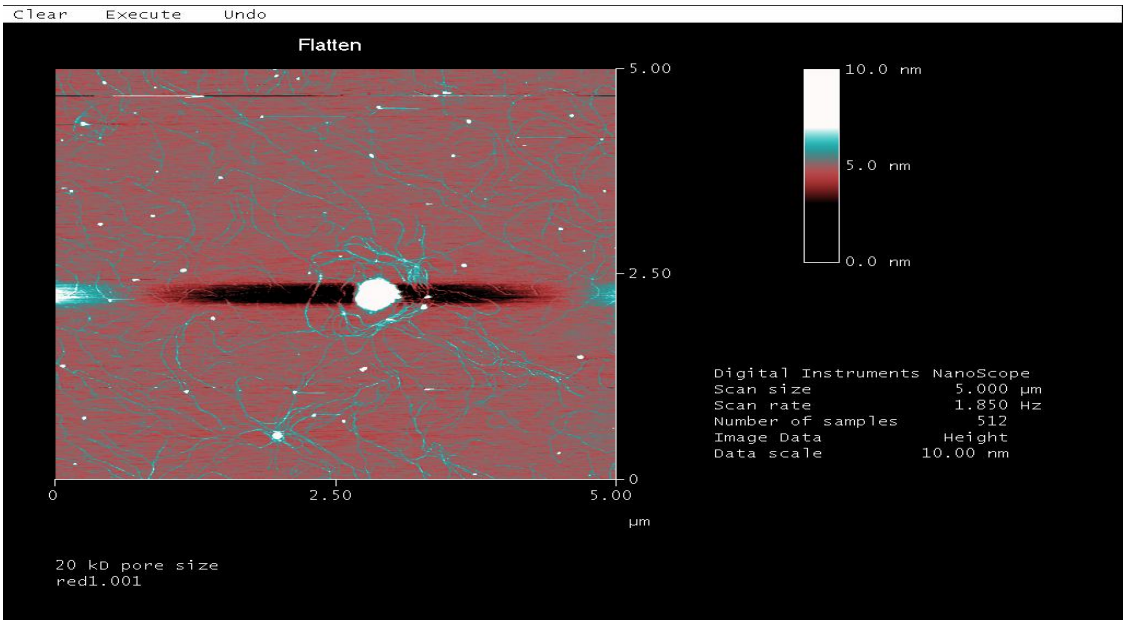

Figure 10: Image from atomic force microscopy (AFM) analysis of a sample from a 20 kD dialysis cell. Perspective looks down from the top of particles 10 nm height.

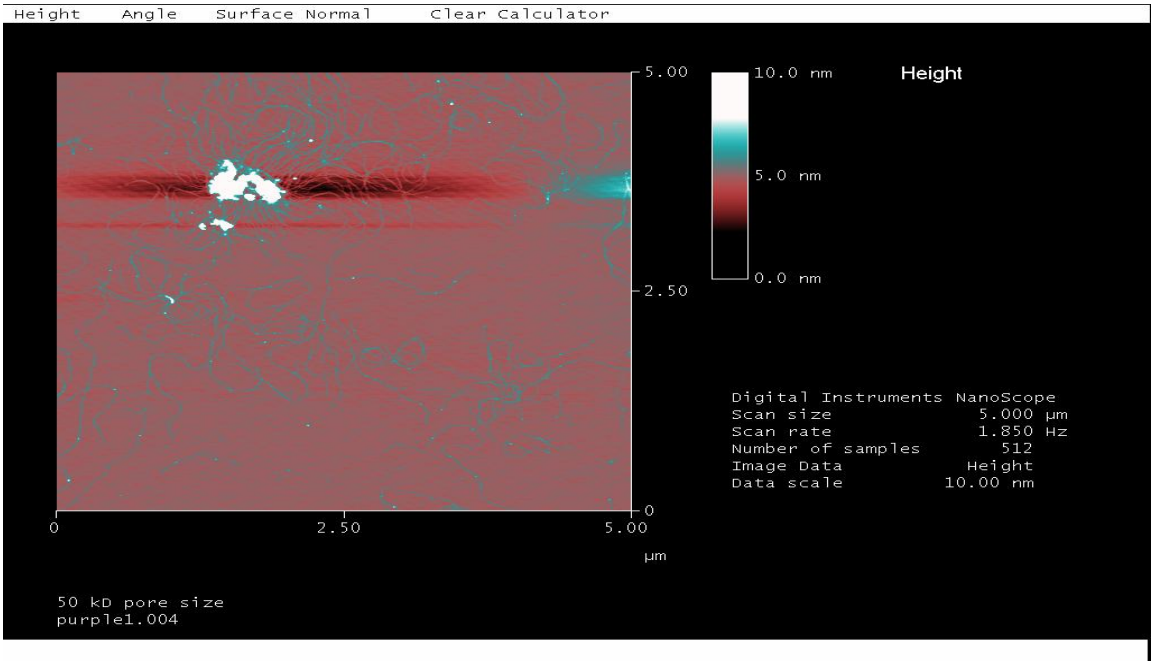

Figure 11. Image from atomic force microscopy (AFM) analysis of a sample from a 50 kD dialysis cell. Perspective looks down from the top of particles 10 nm height.

The TEM samples contain images of both amorphous and crystalline particle formation but no swirling lines of particles can be seen. The 50 kD dialysis cell in particular was easy to find particles with a higher proportion for crystalline structures (Figure 12-13).

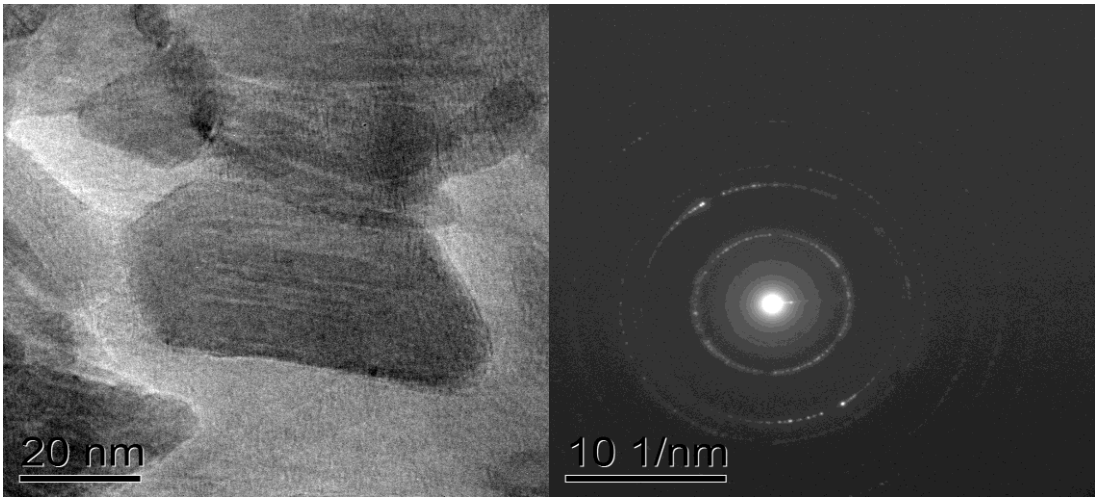

Figure 12. 50 kD dialysis cell Sample 1 Figure 12a: Crystalline TEM image Figure 12b: crystalline diffraction pattern

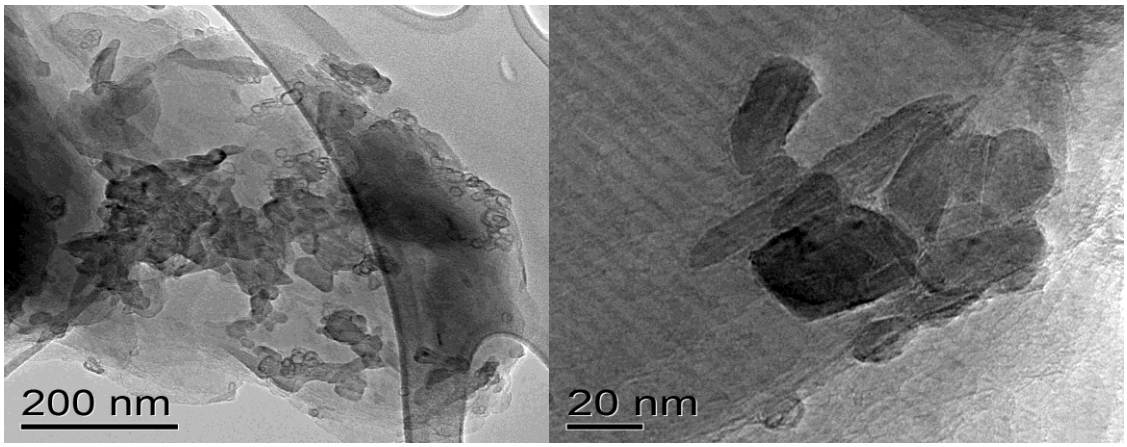

Figure 13: 50 kD dialysis cell Sample 1 Figure 13a. Crystalline TEM images Figure 13b: close up crystalline TEM image

Particle Count Analysis

Particle analysis was done by analyzing grain size mean, number of grains, and maximum gain size at two different threshold heights, 1 nm and 2 nm. Grain size mean is the mean particulate size, number of grains is a count of all particulates on the screen, and the maximum grain size is the size of the largest particulate on the screen. Threshold height is the height at which any particle below the chosen height was not included in the analysis.

The AFM images showed an upward trend of maximum grain size and grain size mean in relation to pore size. The visual inspection of the AFM images was roughly confirmed in the assessment of the particle count analysis shown in Table 2 and 3. The 0.5 kD dialysis cell sample showed a higher count and a larger grain size than expected but when the considered with the visual inspection of the AFM images, these counts were discounted due to the likelihood of poor tip shape on the AFM. Threshold heights of 1 nm and 2 nm were chosen for comparison because of their relation to C60 size, which is approximately 1 nm in diameter. This cut-off as a threshold height eliminated

contamination in the sample but allowed for analysis of singular C60 particles. The 2-nm threshold height then eliminated the singular C60 particles from analysis and analyzed the nano-C60 aggregates. Results of the particle analysis were tabulated for comparison across dialysis membrane pore sizes.

Regression Analysis of Particles Relative to Dialysis Cell Membrane Pore Sizes

Table 2. Particle analysis from AFM using a 1 nm threshold.

Treatment	Grain Size Mean (nm^2)	Number of Grains	Maximum Grain Size (nm^2)
0.5 kD			
0	4590	31	40912
1	1616	70	17642
Average	3130	51	29277
5 kD			
3	157	410	2956
5	605	93	4864
Average	381	252	3910
20 kD			
1	314	1697	121974
4	223	1441	21839
Average	269	1569	71907
50 kD			
2	223	394	14877
4	500	689	158977
Average	362	542	86927
Blank			
0.5 kD	65	19	748
50 kD	30	41	210
Average	48	30	479
Bulk Suspension			
2	244	55	33607
3	1054	107	68588
Average	649	81	51098

Table 3. Particle analysis from AFM using a 2 nm threshold.

Treatment	Grain Size Mean (nm^2)	Number of Grains	Maxi. Grain Size (nm^2)
0.5 kD			
0	7153	10	33664
1	3931	9	10108
Average	5542	10	21886
5 kD			
3	553	5	2289
5	245	14	1144
Average	399	10	1717
20 kD			
1	1908	91	107097
4	794	69	11634
Average	1351	80	59366
50 kD			
2	1330	18	13637
4	3883	42	131416
Average	2607	30	72527
Blank			
0.5 kD	610	1	614
50 kD	11	9	23
Average	311	5	319
Bulk Suspension			
2	465	10	1693
3	1845	35	49739
Average	1155	23	25716

For each dialysis cell suspension the particle size mean, particle number, and maximum size were regressed on membrane pore size. The 1-nm threshold did not show any correlation with the grain size mean or the number of grains (R^2 <0.001). The regression curve for the maximum grain size suggested a positive relationship between pore size and diffusion of the largest aggregates into the cells (R^2 = 0.732) (Figures 14-16).

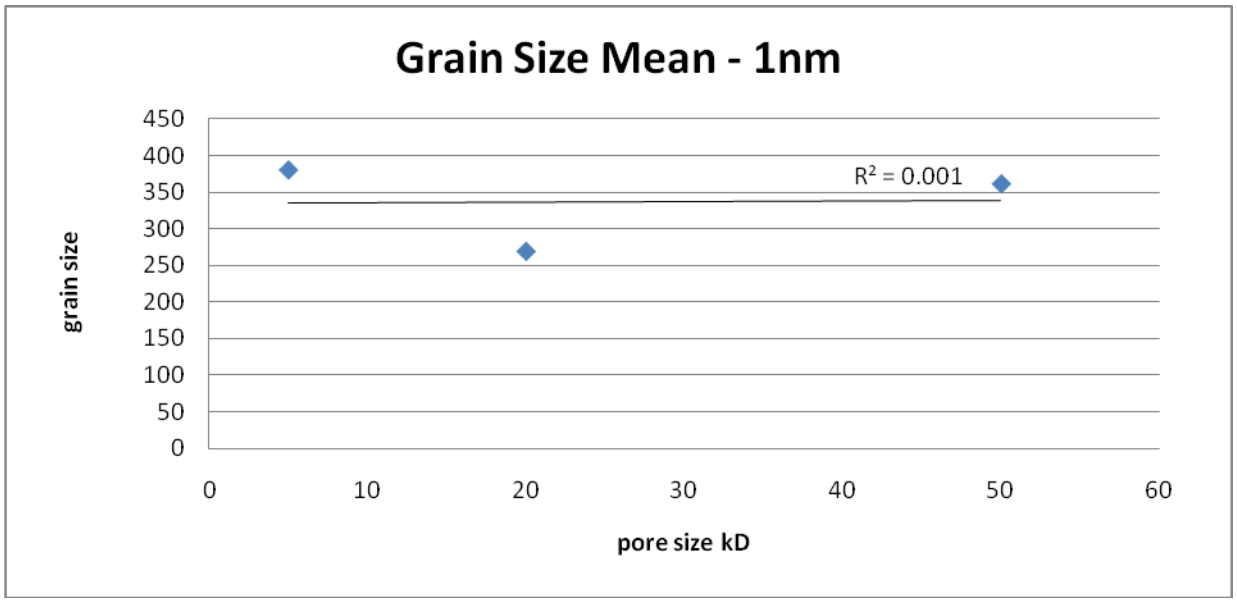

Figure 14. Relationship of grain size to dialysis cell membrane pore size based on AFM analysis at a 1 nm threshold height.

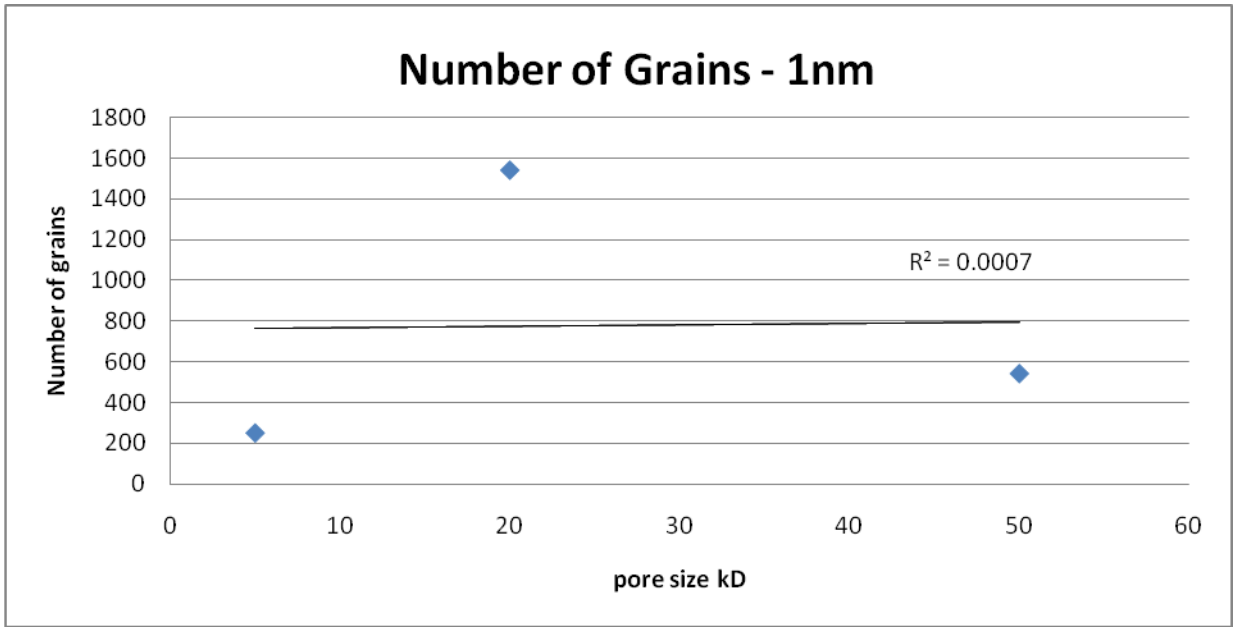

Figure 15. Relationship of number of grains to dialysis cell membrane pore size based on AFM analysis at a 1 nm threshold height.

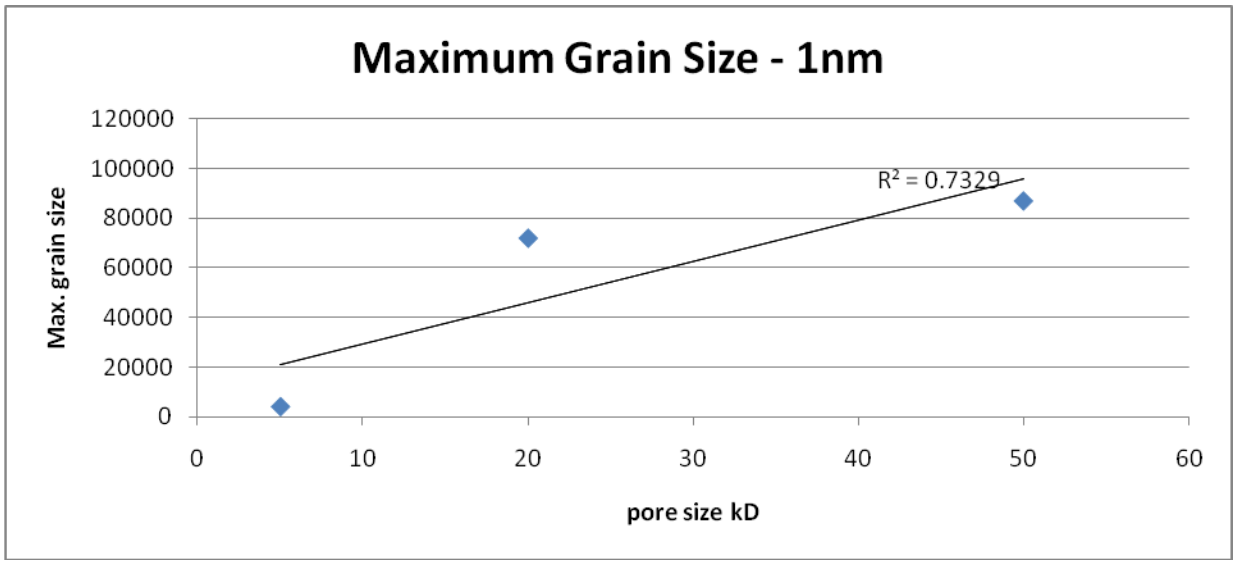

Figure 16. Relationship of maximum grain size to dialysis cell membrane pore size based on AFM analysis at a 1 nm threshold height.

The number of grains diffusing into dialysis cell membranes based on the 2-nm threshold height were not correlated to pore size (R^2=0.08) (Figure 19). However, the regression curves showed better correlations between pore size and the size of diffusing nano-C60 aggregates. The regressions for grain size mean had a R^2 value of 0.987, and maximum size grain regression had a R^2 value of 0.734 (Figures 17 – 19).

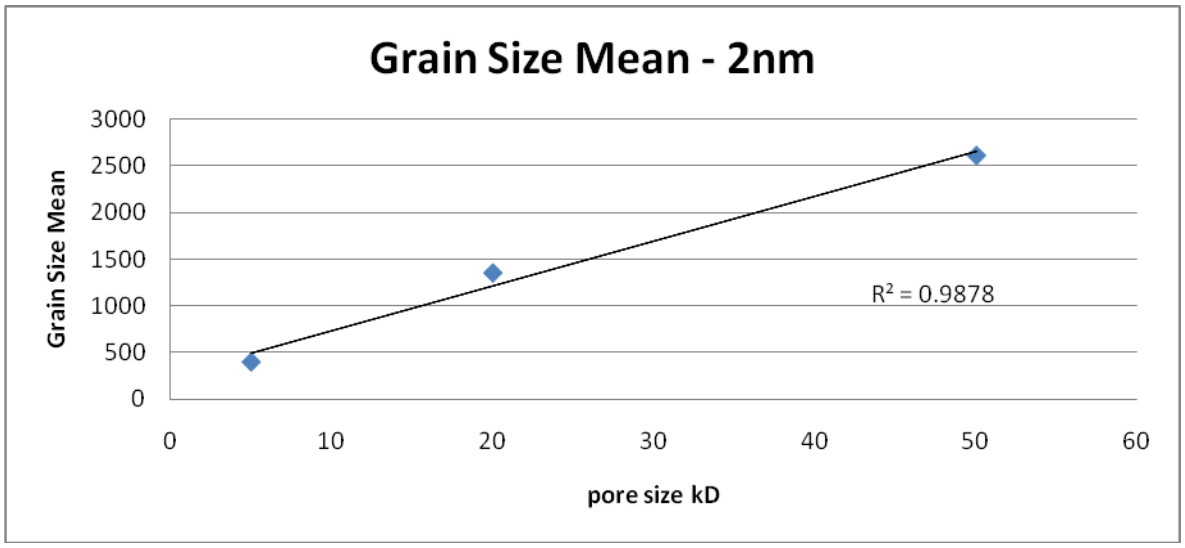

Figure 17: Relationship of grain size to dialysis cell membrane pore size based on AFM analysis at a 2 nm threshold height.

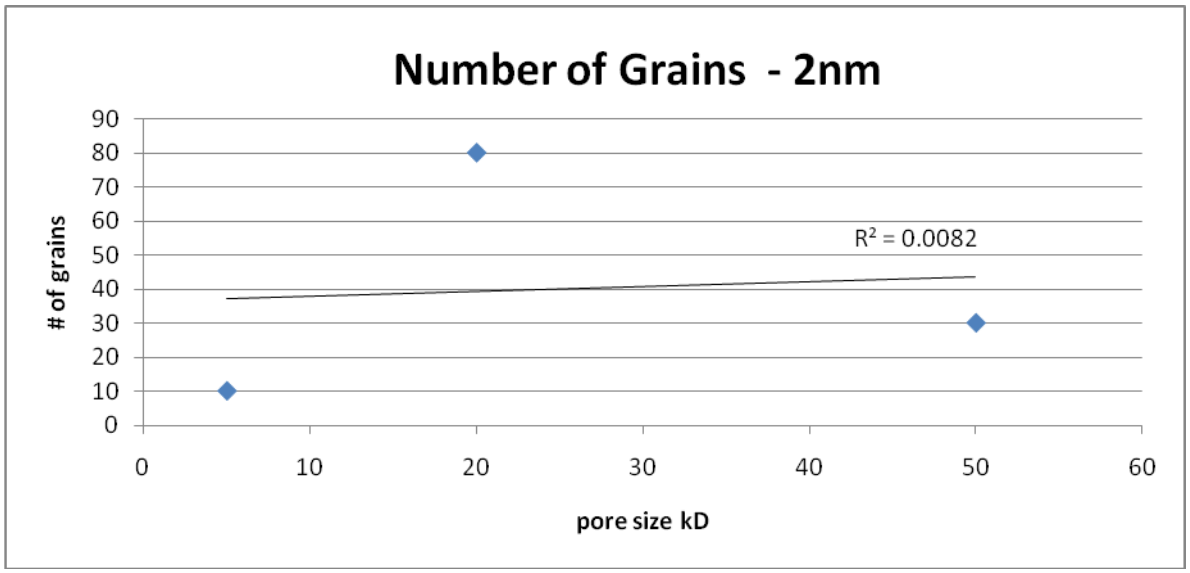

Figure 18: Relationship of number of grains to dialysis cell membrane pore size based on AFM analysis at a 2 nm threshold height.

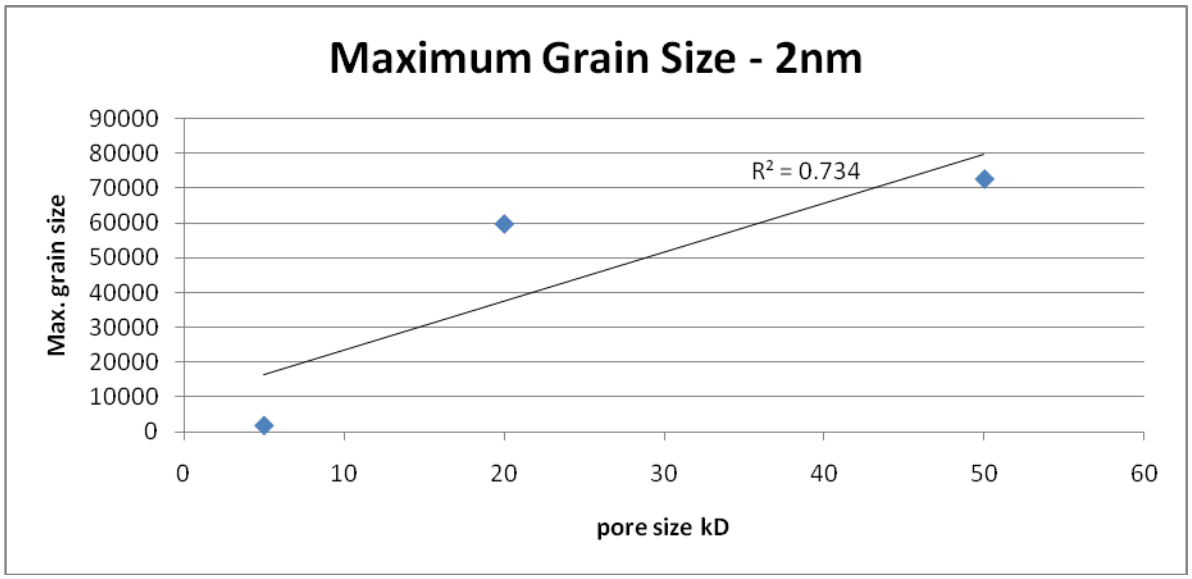

Figure 19: Relationship of maximum grain size to dialysis cell membrane pore size based on AFM analysis at a 2 nm threshold height.

TEM Images

The TEM images further confirmed the presence of particles inside of the dialysis cells. Electron diffraction patterns characterized whether the aggregates had an amorphous or crystalline structure. The crystalline structures were indicated by patterns consisting

of discrete dots (Figures 21, 23, 25), and the amorphous aggregates were characterized by a series of halos arranged in repeated rings (Figures 20, 22, 24). In general, TEM images and diffraction patterns suggested the larger membrane pores favored diffusion of larger aggregate sizes with crystalline structure.

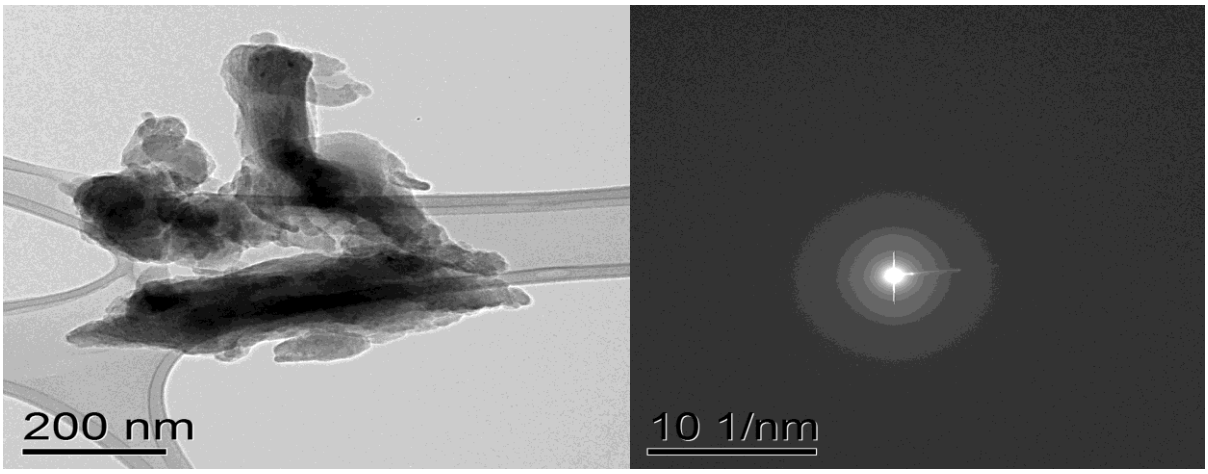

Figure 20. 5 kD dialysis cell sample Figure 20a: Amorphous TEM image Figure 20b: amorphous diffraction pattern

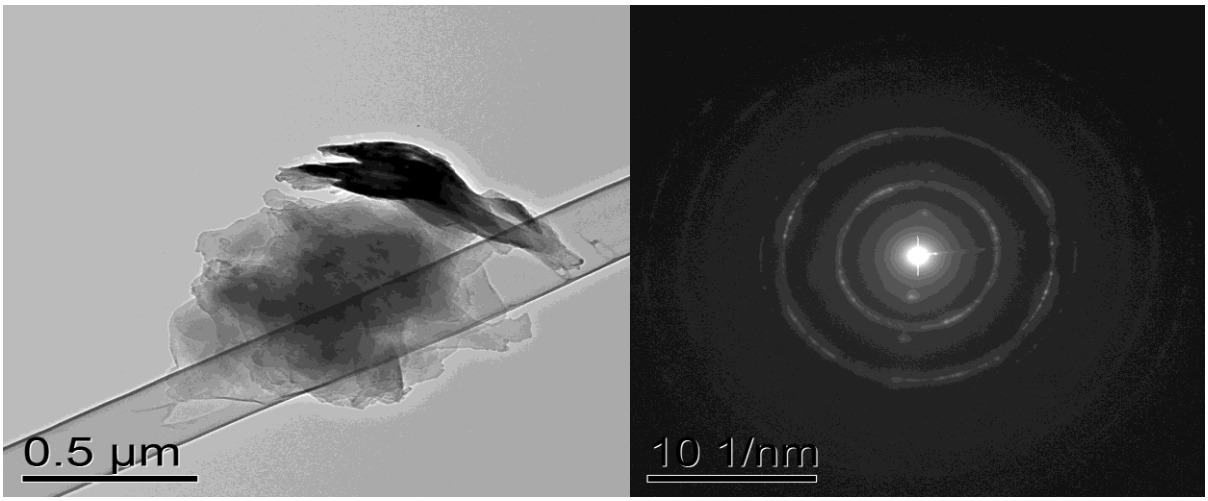

Figure 21. 5 kD dialysis cell sample Figure 21a: Crystalline TEM image Figure 21b: Crystalline diffraction pattern

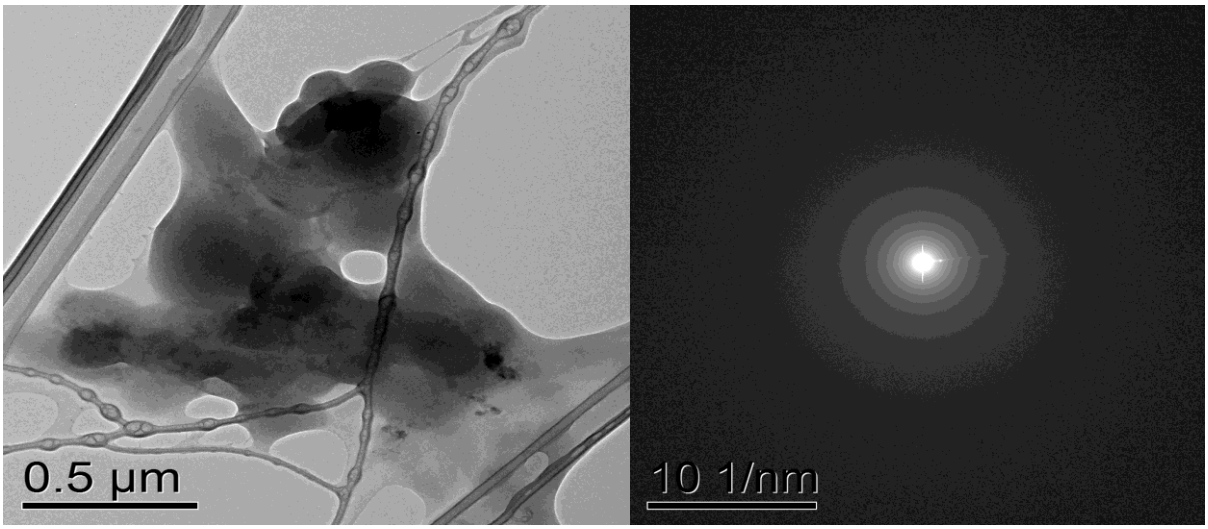

Figure 22. 20 kD dialysis cell sample Figure 22a: Amorphous TEM image Figure 22b: Amorphous diffraction pattern

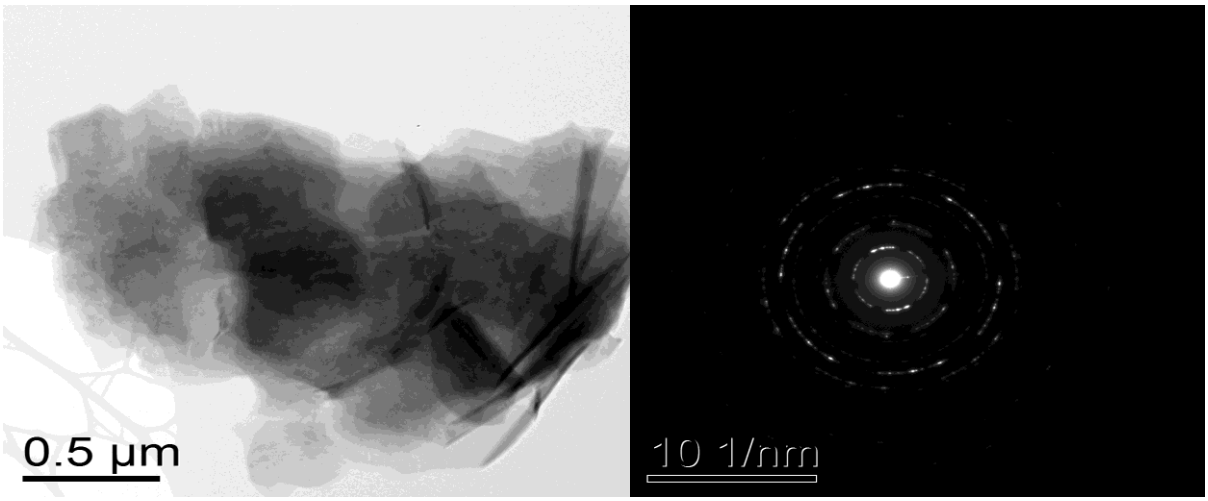

Figure 23. 20 kD dialysis cell sample Figure 23a: Crystalline TEM image Figure 23b: Crystalline diffraction pattern

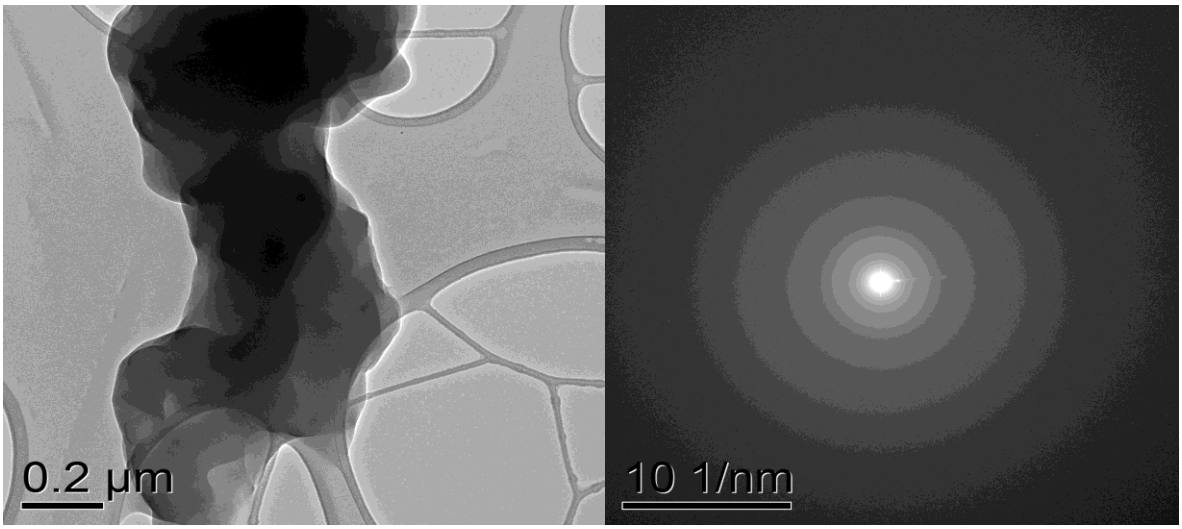

Figure 24. 50 kD dialysis cell sample Figure 24a: Amorphous TEM image Figure 24b: Amorphous diffraction pattern

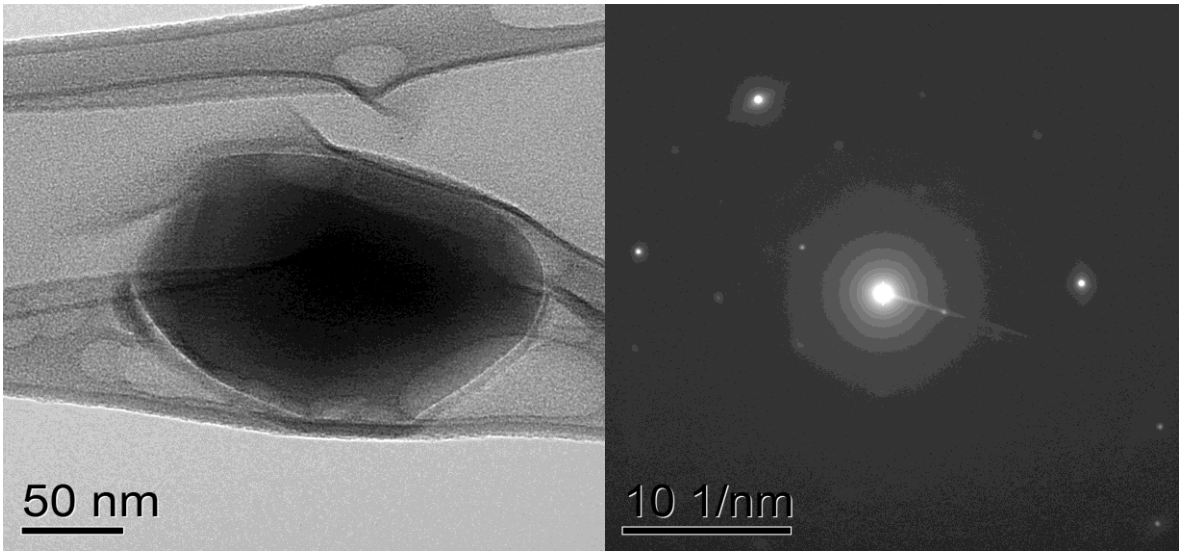

Figure 25. 50 kD dialysis cell sample Figure 25a: Crystalline TEM image Figure 25b: Crystalline diffraction pattern

DISCUSSION AND CONCLUSIONS

The purpose of this study was to examine the movement of nano-C60 aggregates through dialysis cell membranes as surrogates for cell membrane diffusion. Dialysis cell pore sizes were chosen to represent a range of pore sizes that might occur in cell membranes. For example, aquaporins are typically <1 nm diameter, and the smallest dialysis pore used was ~1 nm (Nobelprize.org , 2003). Fullerenes are about 1 nm diameter. Under conditions of stress, for example conditions of lipid peroxidation (Dhawan, 2006) or the presence of bacterial toxins (Clinkenbeard et al. 1989), membrane pore sizes could rapidly increase. The largest dialysis pore size was ~100 nm to account for the possibility that cell membranes under stress may allow diffusion of the nano-C60 aggregates. Because the material is no longer considered nanoscale material at 100 nm, it also begins to lose the novel properties it has at the nanoscale level. The hypothesis was that if the filtration of nano-C60 is related to dialysis cell pore size, then exposing the nano-C60 to smaller dialysis cell pore sizes will filter the nanoparticles from entering the cell.

The observation of swirling lines raises questions about their nature. Are they buckyballs, or are they contaminants that are attracted to the electrophilic structure of the nano-C60 aggregates? Did the lines form because the transport through the cells slowed down the movement of the buckyballs long enough to attach them to each other during the passage through the cells? Would a phospholipid bilayer with pores create the same swirling lines to be attracted to the larger aggregates also?

The experiment has brought up several more issues that can't be addressed with this study, but it does seem that environmental exposure to aggregated C60 buckyballs is related to dialysis cell pore size and exposing the crystals to smaller dialysis cell pore sizes do filter the nanoparticles from entering the cell. Size is an important aspect to toxicological properties and the smaller pore size does filter the size of the aggregate that diffuse through the membranes, but it seemed that the aggregates were still forming within the cellular membrane. The observations of greater than expected particle sizes in some dialysis cells suggest that the buckyballs continued aggregating within the cells. UV/VIS analysis suggested that aggregates in the constantly stirred bulk solution formed larger colloids. Thus, continued aggregation of buckyballs could plausibly be hypothesized to be occurring inside the cells. Especially interesting are the formation of the swirling lines. The next aspect to consider is the physical nature of the swirling lines, which do not appear in the bulk material, and how they are formed inside the cells.

BIBLIOGRAPHY

Alargova, R; Degushi, S; Tsujii, K. 'Stable Colloidal Dispersion of Fullerenes in Polar Organic Solvents.' *Journal of American Chemical Society*, (2001), 123, 10460-10467.

Andrievsky, GV; Klochkov, VK; Karyakina, EL; Mchedlov-Petrossyan, NO. 'Studies of Aqueous Colloidal Solutions of Fullerenes C60 by Electron Microscopy.' *Chemical Physics Letters*. (1999), 300, 392-396.

Bouchard,D; Ma, X; Isaacson, C. 'Colloidal Properties of Aqueous Fullerenes: Isoelectric Points and Aggregation Kinetics of C60 and C60 Derivatives' *Environmental Science & Technology.(* 2009) *43* (17), 6597-6603.

Dhawan, A; Taurozzi, JS; Pandey, AK; Shan, WQ; Miller, SM; Hashsham, SA; Tarabara, VV. 'Stable Colloidal Dispersions of C60 Fullerenes in Water: Evidence for Genotoxicity'. *Environmental Science Technology*. (2006), 40, 7394-7401

Farnsworth, M; Fernandez, M; Sabbatini, L. 'Buckyballs: Their history and discovery' (2005). URL:http://cnx.org/content/m14355/latest/. Accessed 11-2009.

Fortner, JD; Lyon, DY; Sayes, CM; Boyd, AM; Falkner, JC; Hotze, EM; Alemany, LB; Tao, Yl; Guo, W; Ausman, KD; Colvin, VL; Hughes, JB. 'C60 in Water: Nanocrystal Formation and Microbial Response.' *Environmental Science Technology*, (2005), 39, 4307-4316.

Hungerbuhler, H;Guldi, DM. and Klaus-Dieter, A. 'Incorporation of CW into Artifical Lipid Membranes.' *Journal of American Chemical Society*. (1993),115, 33863387.

Kamat, JP; Devasagayam, TPA; Priyadarsini, KI; Mohan, H. 'Reactive oxygen species mediated membrane damage induced by fullerene derivatives and its possible biological implications'. *Toxicology* 155 (2000), 55–61

Kroto, HW; Heath, JR; O'Brien, SC; Curl RF; Smalley, RE. 'C_{60}: Buckminsterfullerene' *Nature* (1985), 318: 162–163.

Locke, W. 1996. Buckminsterfullerene, C60. URL:http://www.bristol.ac.uk/Depts/Chemistry/MOTM/buckyball/c60a.htm . Accessed 11-2009.

Magrez, A; Kasas, S; Salicio, V; Pasquier,N ; Seo, JW; Celio, M; Catsicas, S; Schwaller, B; Forro, L. 'Cellular Toxicity of Carbon-Based Nanomaterials'. *Nanoletters* 6 (2006), 1121-1125.

Nanosciences Instruments, 2008. URL:http://www.nanoscience.com/education/AFM.html. Accessed 11-2009.

Nanotox.info, 2008. URL:http://www.nanotox.info/protocols.html. Accessed 4-2008.

Nobelprize.org , 2003. URLhttp://nobelprize.org/nobel_prizes/chemistry/laureates/2003/. Accessed 11-2009.

Nobelprize.org , 2006.
URL:http://nobelprize.org/nobel_prizes/chemistry/laureates/1996/. Accessed 11-2009.

Nobelprize.org, 2009.
URL:http://nobelprize.org/educational_games/physics/microscopes/tem/index.html.
Accessed 11-2009.

Oberdorster, E; Zhu, S; Blickley, TM; McClellan-Green, P; Haasch, ML. 'Ecotoxicology of carbon-based engineered nanoparticles: Effects of fullerene (C60) on aquatic organisms'. *Carbon 44* (2006) 1112–1120

Qiao, R; Roberts, AP; Mount, AS; Klaine,SJ; Ke, PC. 'Translocation of C60 and Its Derivatives Across a Lipid Bilayer'. *Nanoletters*, 2007, Vol. 7 No. 3, 614-619.

Spurlin, TA; Gewirth, AA. 'Effect of C60 on Solid Supported Lipid Bilayers'. *Nanoletters*, 2007, Vol. 7 No. 2, 531-535.

Sayes, CM; Gobin, AM; Ausman, KD; Mendez, J; West, JL; Colvin, VL. (2005). 'Nano-C60 cytotoxicity is due to lipid peroxidation'. *Biomaterials*, Vol. 26, Issue 36, December 2005, 7587-7595.

Sayes, C. M.; Fortner, J. D.; Guo, W.; Lyon, D.; Boyd, A. M.; Ausman, K. D.; Tao, Y. J.; Sitharaman, B.; Wilson, L. J.; Hughes, J. B.; et al. (2004). 'The Differential Cytotoxicty of Water-Soluble Fullerenes.' *Nanoletters.* 2004, Vol. *4*, 1881.

SES Research URL: http://www.sesres.com/FullerenesPrices.asp Accessed 4-2009.

Tang, YJ; Ashcroft, JM; Chen, D; Min, G; Kim, CH; Murkhejee, B; Larabell, C; Keasling, JD; and Chen, FF. (2007) 'Charge-Associated Effects of Fullerene Derivatives on Microbial Structural Integrity and Central Metabolism.' *Nanoletters*, 2007, Vol. 7, No. 3, 754-760.